POLITECNICO DI TORINO
Repository ISTITUZIONALE

Overload Capability of Multiphase Machines Under Normal and Open-Phase Fault Conditions: A Thermal Analysis Approach

Terms of use:

Publisher copyright

(Article begins on next page)

26 April 2024

Overload Capability of Multiphase Machines under Normal and Open-Phase Fault Conditions: a Thermal Analysis Approach

A. Boglietti, R. Bojoi, S. Rubino, M. Cossale

Dipartimento Energia "G. Ferraris"
Politecnico di Torino, Torino, Italy

Abstract— **Multiphase drives are convenient for high power/high current applications as they allow the reduction of the phase current for given rated power and phase voltage. Due to their redundant structure, the multiphase drives have intrinsic open-phase fault-tolerant operation capability. This situation may happen when one or more power electronic units are turned off after a fault event, and the drive configuration allows phase disconnection. In this case, the healthy machine phases can be overloaded to keep the torque constant and without any pulsations. The goal of the work is the evaluation of the thermal parameters of the stator windings of multiphase machines to be used in the analysis of both short thermal transients and steady-state operation, during normal and open-phase faults. The approach has general validity and can be applied to any AC multiphase machine having a distributed winding configuration. The prototype used for the experimental tests is an asymmetrical twelve-phase induction machine, having four three-phase stator sets with isolated neutral points. The stator windings thermal model is obtained experimentally, by considering the mutual heat exchange phenomena among the windings when one or more winding sets are disconnected. This thermal model allows at evaluating the proper machine overloading for short thermal transients and steady-state operation in case of open-phase faults.**

Keywords—multiphase machines, thermal model, identification, open-phase fault operation.

I. INTRODUCTION

An electrical drive is defined as multiphase when the number of phases n of the electrical machine is higher than three ($n>3$) [1,2]. Multiphase drives are interesting for high power or high current applications as they allow the reduction of the current per phase for given rated power and without increasing the voltage per phase. Besides, when compared to their three-phase counterparts, they have reduced torque pulsations and possess inherent fault-tolerant capability due to their redundant structure.

Currently, the multiphase drives are the state-of-the-art for electrical ship propulsion and a promising solution for other reliability-critical applications, such as railway traction, Hybrid/Electrical Vehicles (HEV/EV), wind power generation, More Electric Engine (MEE) and More Electric Aircraft (MEA) applications [1]-[5]. The load capability of any electrical machine depends on its thermal behavior and the cooling system. The thermal overload of the machine may cause severe damages to the winding insulation, causing accelerated thermal-aging and premature failures. For this reason, the thermal analysis assumes an even more critical role for the electrical machines used in applications with short-time load and overload operations, such as automotive and aerospace applications.

Due to their redundant structure, the multiphase drives have intrinsic open-phase fault-tolerant operation capability. The open-phase fault may happen when one or more power electronic units are turned off after a fault event, and the drive continues to operate with machine units that are opened. In this case, the healthy machine phases can be overloaded to keep the torque constant and without any pulsations. The literature reports different solutions related to the drive control to reduce the torque pulsations in case of open phase faults [6-8] or to keep the torque as high as possible [9]. The open-phase and three-phase short-circuit operations for a symmetrical six-phase induction machine are provided in [10,11], focusing on the winding configurations that influence the machine's magnetic conditions in case of a fault.

According to the authors' best knowledge, the literature offers limited references regarding the thermal behavior of multi-phase machines to predict the load behavior for both healthy and open-phase conditions [10], [12,13].

Therefore, the goal of the work is the evaluation of the thermal parameters of the stator windings of multiphase machines to be used in the analysis of short thermal transients in normal and open-phase faults. This work is an extension of [14], where preliminary analysis and results have been presented.

The thermal parameters allow at obtaining the proper overload capability of the healthy phases in case of open-phase faults. The approach has general validity and can be applied to any AC multiphase machine. The prototype used for the experimental tests is an asymmetrical twelve-phase induction machine prototype, having four three-phase stator sets with isolated neutral points. The paper is organized as follows. Section II presents the multiphase machines configurations and the machine prototype used for the tests. Section III describes the adopted procedure to identify the thermal parameters for different open-phase configurations, while Section IV contains the experimental results for transient and steady-state conditions.

II. MULTIPHASE MACHINE CONFIGURATION

Multiphase machines are divided into symmetrical or asymmetrical machines, depending on the electrical displacement between two adjacent phases [5]. For a given number of phases n ($n>3$), the symmetrical machine has a spatial displacement γ of $360/n$ electrical degrees between the magnetic axes of two consecutive phases. As an example, a five-phase machine has a spatial displacement γ of 72 electrical degrees between two consecutive stator phases.

When the number of phases is an even number or an odd number that is not a prime number, the machine can be seen as m sets having a phases each [2]. Typically, $a=3$ (three-phase sets), $m=2,3,4,5...$, and, the spatial displacement between the first phases of two consecutive sets is $180/n$ electrical degrees. As an example, an asymmetrical six-phase machine has $m=2$ three-phase sets ($a=3$), and the spatial displacement between the first phases of the two three-phase sets is 30 electrical degrees.
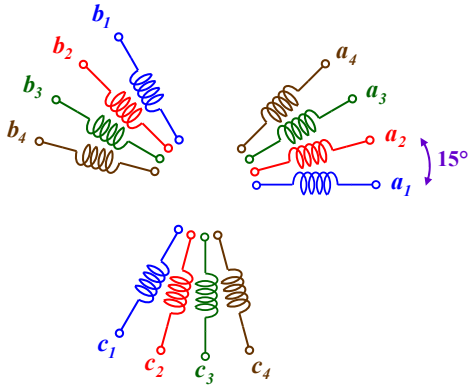
Fig. 1. Asymmetrical 12-phase induction machine configuration.
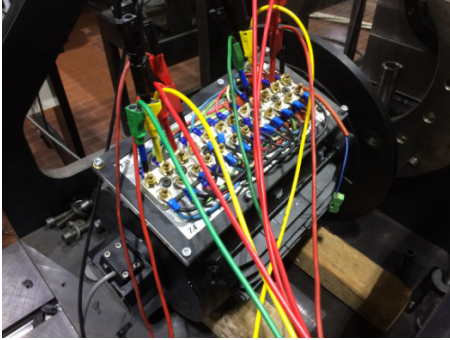

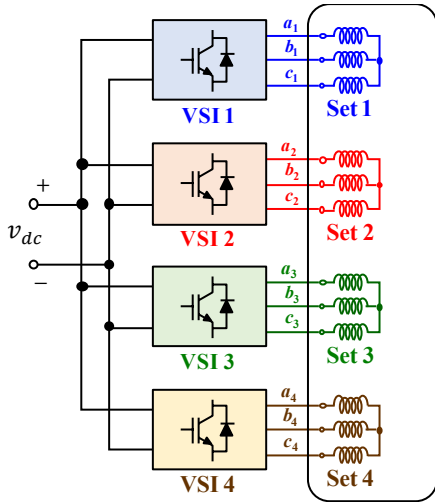Fig. 2. View of the multiphase machine under test.

Fig. 3. Drive configuration with multiple three-phase units supplying three-phase stator sets with isolated neutral points.

An asymmetrical twelve-phase machine has m=4 three-phase sets (a=3), and the spatial displacement between the first phases of two consecutive sets is 15 electrical degrees.

The machine used in this investigation is an asymmetrical twelve-phase induction generator, rated 10 kVA at 200 Hz. The machine stator winding configuration is shown in Fig. 1, while a view of the machine is shown in Fig. 2. The machine rated data are provided in the Appendix.

The machine has an entirely reconfigurable winding phase since the terminals of all twelve phases are available in the connector box. Moreover, it should be remarked that the machine under test uses single-layer distributed windings with 1 slot/pole/phase.
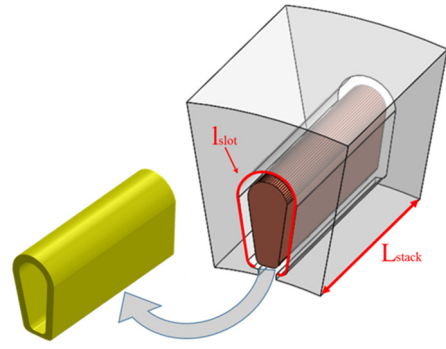

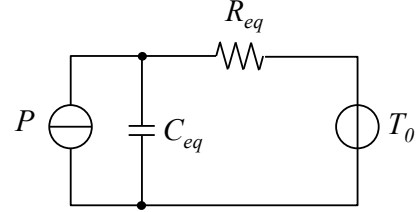Fig. 4. A schematic representation of a single stator-winding slot.

Fig. 5. First-order winding thermal modeling network.

A feature of this winding configuration is that the end windings of phases belonging to one three-phase set are in thermal contact with end windings belonging to other three-phase sets.

During the normal operation, the four three-phase stator sets have isolated neutral points, and they are supplied by three-phase inverter units, as shown in Fig. 3. In case of fault related to one inverter module, the corresponding three-phase set is disconnected, thus behaving as an open three-phase winding set.

III. THERMAL MODELING AND TEST PROCEDURE

The thermal modeling of electrical machines covers a variety of simplified or sophisticated networks aimed to describe the thermal transfer from the various regions of the machine body to the ambient [15]. However, the stator winding region is usually attributed as being the main heat source within the machine body, thus imposing the most important temperature limit. Therefore, an accurate assessment of heat path winding-to-stator is crucial to assess a high-reliability thermal analysis of electrical machines. This is particularly relevant in those applications operating in transient overload duty or fault conditions such as the case under study.

As known, the stator winding insulation system is a randomly distributed composite with slot liner, impregnation, and air cavities, and its thermal behavior depends on several factors such as winding arrangement, impregnation technique, and material physical parameters.

In this regard, the authors modeled the copper winding plus insulation as a homogeneous concentration of the conductor material in the middle of the slot that is surrounded by an equivalent impregnation and insulation materials. It is worth noticing that this model approach is suitable for both, distributed and concentrated windings, no matter if they are three-phase or multiphase [16,17]. Fig. 4 presents a close up on a single stator-winding slot with related insulation, to be modeled using two thermal parameters: the equivalent thermal resistance and thermal capacitance.

The former represents the heat transfer between stator copper and iron lamination, while the latter represents the overall thermal capacitance of the winding system (conductor and insulation). However, the thermal parameters associated with this area are challenging to be assessed, and the adoption of pure material properties as input data for the analytical computation returns inaccurate parameter values. The experimental assessment is a commonly used approach to overcome the lack of information. In this way, reliable values of the thermal parameters are obtained.

Therefore, the short-duty transient thermal test has been proposed by the authors in [18] to emulate an isothermal condition for the laminated stator core pack. It means that the stator winding can be considered an adiabatic system, while the stator core temperature remains constant during the test. The winding system is modeled as a simple first-order thermal network illustrated in Fig. 5, where R_{eq} and C_{eq} are the winding equivalent thermal resistance and the equivalent thermal capacitance, respectively. The equivalent winding thermal resistance and capacitance can be assessed using a transient test with dc excitation.

The method consists of heating the stator windings of the machine by the injection of dc current. In this way, the heat source is localized in the windings, while neither iron losses nor mechanical losses are generated. Before testing, the machine has to be in isothermal condition with the external environment. Moreover, it is important to measure the resistance of the phase configuration. It is assumed that the isothermal operating condition for the stator assembly is satisfied for an average rise of the stator temperature up to 1°C. Alternatively, when the test duration is equal to the winding time constant. During the dc test, the phase voltage and current must be logged with a sampling frequency in the range of 1-5 Hz. The instantaneous winding temperature is assessed from the winding resistance variation using the material temperature coefficient.

$$T = \frac{R_T}{R_0} \cdot (234.5 + T_0) - 234.5 \qquad (1)$$

where: R_0 is the winding resistance at the temperature T_0, R_T is the winding resistance at the temperature T; 234.5 is the copper temperature coefficient. Since the winding is considered in an adiabatic condition, T_0 is the temperature of the component next to the winding (lamination). However, because the test starts with the motor under test at the ambient temperature, T_0 corresponds with both ambient temperature and those of the component next to the winding. Once the time variation of the winding temperature has been obtained, the thermal capacitance of the winding system can be computed through the electrical energy provided during the test ($W = v_{dc}(t) \cdot i_{dc}(t) \cdot t$). In particular, by fitting the energy as a function of the winding temperature variation with linear regression, the value of the thermal capacitance C_{eq} can be directly obtained using (2).

$$C_{eq} = \frac{dW}{dT} \qquad (2)$$

The thermal network of Fig. 5 is described by a first-order time-differential equation, and (3) represents its mathematical solution. Regarding this, P is the power loss while the indices k and 0 refer to the generic time instant and the initial condition, respectively.
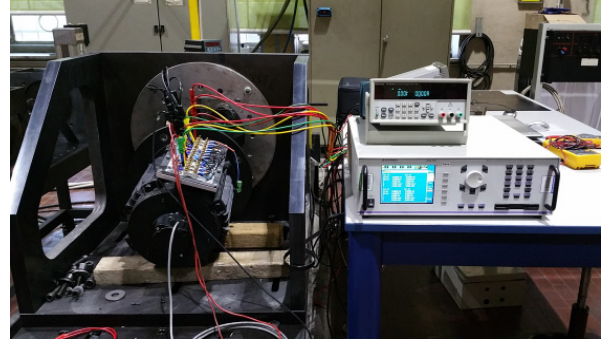

Fig. 6. Thermal test bench for the multiphase machine.

In (3) all variables are known, and the equivalent thermal resistance R_{eq} can be found by minimizing the squared deviation between the measured temperature and the one obtained using the mathematical model (3).

$$T_k = T_{k-1} + \left(T_0 + R_{eq} \cdot P_{k-1} - T_{k-1}\right) \cdot \left(1 - e^{-\frac{t_k - t_{k-1}}{R_{eq} \cdot C_{eq}}}\right) \qquad (3)$$

The product of the obtained thermal parameters, namely the stator winding thermal time constant τ, can be therefore used to predict the temperature rise during an overload or the time duration of the overload itself. In the considered case study, the thermal time constant associated with each three-phase set configuration can be used to estimate the thermal behavior during healthy and open fault conditions.

IV. EXPERIMENTAL RESULTS

The experimental method previously described has been then adopted for estimating the thermal parameters of the investigated multiphase machine. The thermal test bench is shown in Fig. 6. The evaluation of the equivalent thermal resistances and capacitances has been performed with a transient dc test and steady-state dc test, as described in the next subsections.

A. Parameters evaluation from dc transient test

The winding thermal resistance and the winding thermal capacitances have been computed by testing the machine with four sets, three sets, two sets, and one set configuration, respectively. The set configurations are reported in Fig 7, where each configuration is clearly emphasized. The reason for testing the machines in these configurations is to find potential mutual thermal effects among the winding sets and to understand the weight of these effects on the global thermal behavior of the machine.

For each phase configuration, thermal capacitance and thermal resistance have been assessed using the procedure previously described. The voltage and current measurements have been performed using the Zimmer LMG500 power analyzer. The sampling frequency used for logging has been set at a constant value of 5 Hz. It is important to highlight that a higher sample rate increases the number of data but not the accuracy of the results. The power supply has consisted of the Elektro-Automatik EA-PS 2042-20B. All tests have been performed by setting the power supply in voltage control mode with current limitation enabled.

From Fig. 8 to Fig. 12, the thermal energy versus the temperature variation is reported for all possible configurations.
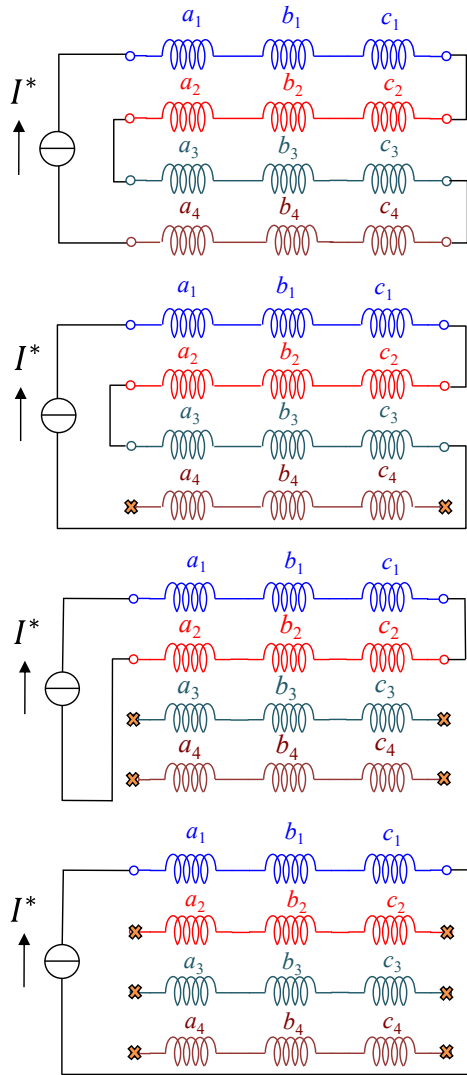
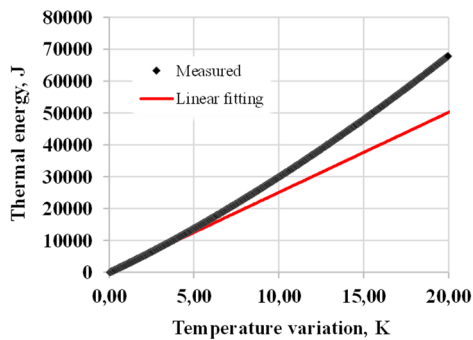Fig. 7.   Sets configurations for the determination of the thermal parameters.

Fig. 8.   Extended transient representing winding thermal energy versus temperature variation (four active winding sets).

Fig. 9.   Winding thermal energy versus temperature variation (four active winding sets).

Fig. 10. Winding thermal energy versus temperature variation (three active winding sets).

Fig. 11. Winding thermal energy versus temperature variation (two active winding sets).
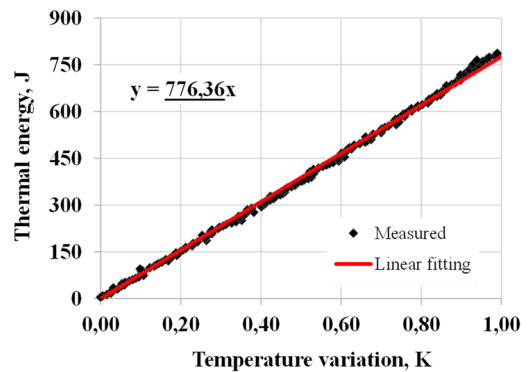
Fig. 12. Winding thermal energy versus temperature variation (one active winding set).

The adiabatic condition of the winding is valid for a temperature rise up to 0.8-1 K, where the energy trend is linear, as in Fig. 8 that shows the extended thermal transient for the four-sets configuration. The temperature rise up to 1 K is a good practical recommendation.

It is well evident that when the thermal energy versus the temperature variation is linear, the windings are in the adiabatic condition and the thermal model of Fig. 5 can be adopted. After the linear trend, the derivative of the thermal energy increases because other thermal capacitances came into play, and the first-order thermal model of Fig. 5 cannot be used anymore.
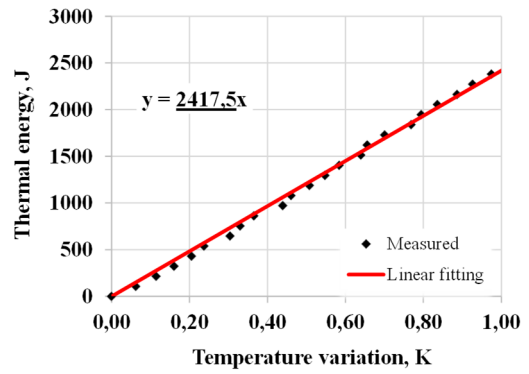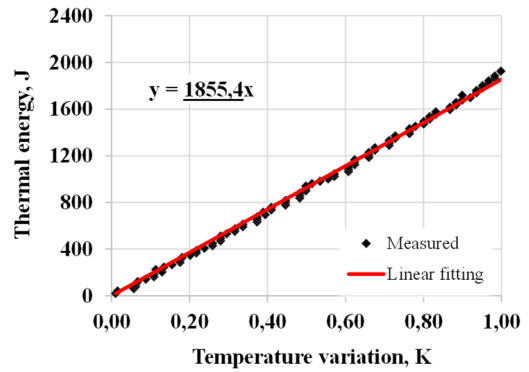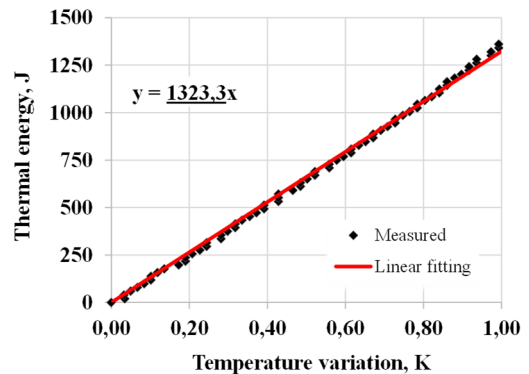
Fig.13. Winding temperature variation during short thermal transient (four active winding sets).

Fig.14. Winding temperature variation during short thermal transient (three active winding sets).
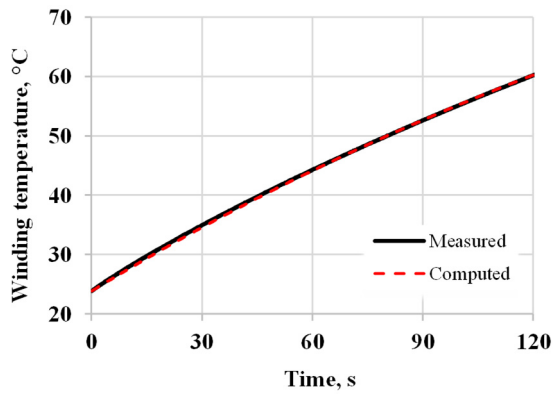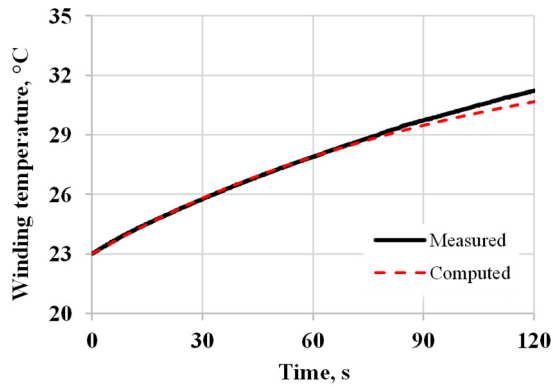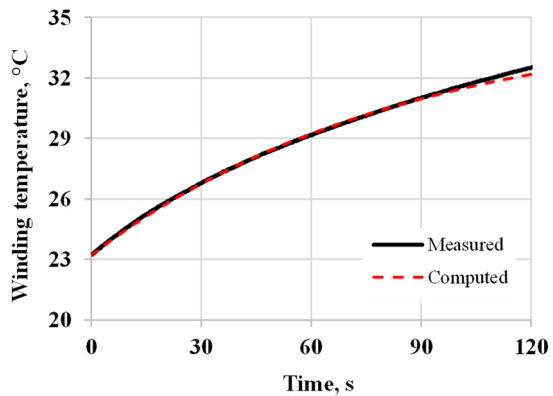

Fig. 15. Winding temperature variation during short thermal transient (two active winding sets).
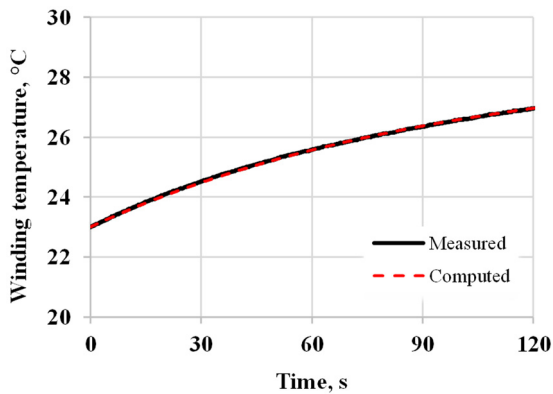

Fig. 16. Winding temperature variation during short thermal transient (one active winding set).
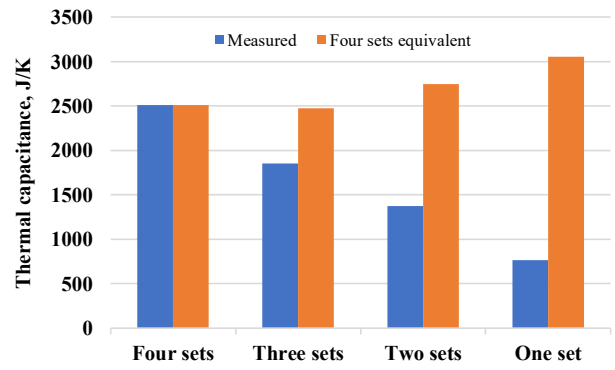

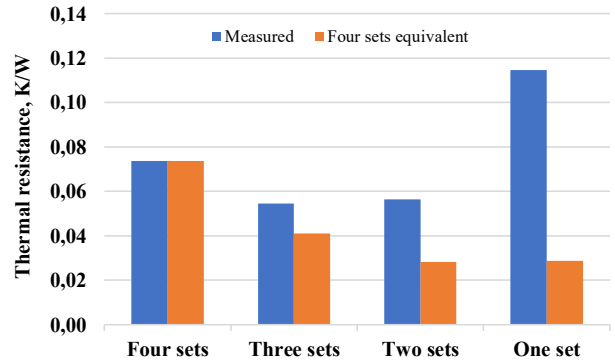Fig. 17. Thermal capacitances for the four-sets configurations.

Fig. 18. Thermal resistances for the four-sets configurations.

Regarding Figs. 9-12, it is well evident the linear trend of the thermal energy versus the temperature variation as expected for an adiabatic system [18].

The winding temperature transient is shown from Fig. 13 to Fig. 16 for the four configurations. It is well evident the excellent agreement between the computed temperatures and the measured ones, confirming the validity of the first-order thermal model for short thermal transient [18] (for this machine 120 seconds long). Since the thermal parameters (R_{eq} and C_{eq}) are not dependent on the joule losses, the short transient can be performed at any current value (paying attention to avoid damage to the windings). For this reason, the temperatures at 120 s can be different, as shown in Figs. 13-16.

The obtained thermal parameter values are reported in Fig. 17, and Fig. 18 respectively. In Fig. 17, the A bars represent the measured winding thermal capacitances for each set configuration. It is well evident that the values of these capacitances become lower with the reduction of the number of active three-phase sets. This result is reasonable because the reduction of the set corresponds to a reduction of the copper and insulation mass involved in thermal transient.

The B bars from Fig. 17 are the values of the winding thermal capacitances for each set configuration reported to the four winding sets configuration. Since the thermal capacitances are proportional to the involved material mass, the four-set equivalent thermal capacitances have been computed by multiplying the three sets value by 4/3, the two-winding set value by 2 and the one winding set value by 4. It is important to highlight that the equivalent thermal capacitance values are very close to the value obtained with four winding sets, and with a maximum error that is below 20%. Considering the complexity of the thermal tests, the authors consider these results as extremely positive.
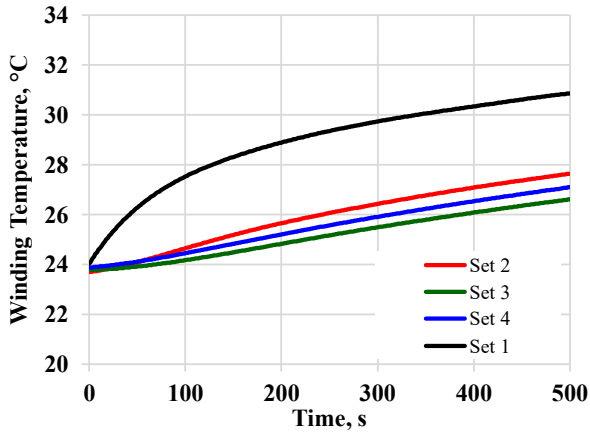
Fig. 19. Mutual heat exchange between a supplied set and the other disconnected sets.

Fig. 20. Thermal time constant of stator winding region.

An outcome of these tests is that the thermal capacitances of the set configurations can be computed using just one set when some configurations cannot be thermally tested in the right way. This result could allow a reduction of the thermal tests to be performed on the machine. For example, if the multiphase machine cannot be tested with all sets due to physical constraints, then the test can be performed with only one set.

The winding thermal resistance values are reported in Fig. 18 for each winding set, where the A bars show the value measured for each set condition. It is noted that using the thermal resistance of the four winding sets as the reference value, the one obtained with one winding set is about 1.6 times higher. This value is far below the expected ratio of 4, considering the reduction of surface for the heat exchange.

Still looking at Fig. 18, the bars that represent the two and three set configurations show values that are lower than the one obtained with the four-set configuration. At a first analysis, this could seem unreasonable since a reduction of the heat exchange surface between winding and lamination should produce an increase of the thermal resistance value and not vice versa.

The answer to this trend is in the mutual heat exchange between the active winding set and the inactive ones. Since the machine under test has distributed windings, there is physical contact between the end-winding of each three-phase set. This results in an additional thermal path between the active set and the inactive ones, thus influencing the equivalent thermal resistance of each set according to the configuration. In other words, the inactive set helps the others to dissipate the produced heat, allowing the machine overload. These considerations are confirmed by looking at the B bars of Fig. 18. Like the case of thermal capacitance, the B bar values show the equivalent four winding set thermal resistance computed starting from the three, two, and one set values. In particular, the equivalent four winding set thermal resistance has been obtained by dividing the one-set value by 4, the two-sets value by 3, and the three-sets one by 4/3.

It is well evident that the equivalent four-set thermal resistance values decrease with the reduction of the sets number, thus confirming the mutual heat exchange phenomena among the sets. To further investigate this phenomenon, a specific test has been performed with one active set, while the others have been disconnected.
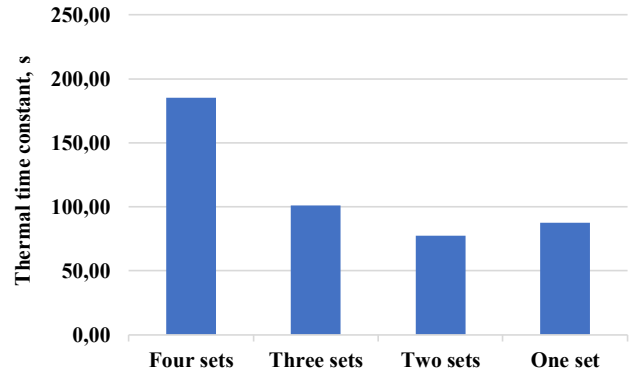
The measured temperatures of the sets winding are shown in Fig. 19. It is well evident that in short transient conditions, the increase of the winding temperatures of the disconnected sets is not negligible, with an increase of 2°C compared to 6 °C of the supplied set.

Finally, the thermal time constants of the stator winding can be considered as the most representative outcomes from the identification of the transient thermal parameters. Fig. 20 shows the obtained values for each winding set configuration. Looking at the picture, it can be noted a large difference between the value associated with the normal configuration case (four-sets) compared to the ones related to open-fault cases. Therefore, considering an overload condition such that the winding losses are equal for the investigated three-phase set configurations, the winding thermal limit will be reached in 185s, 101s, 77s, 88s for four-sets, three-sets, two-sets and one-set respectively.

B. Parameters evaluation from dc supply steady-state test

In addition to the transient thermal tests, the machine has been tested at thermal equilibrium using dedicated thermal tests with dc excitation. In the specific case study, the tests are aimed to evaluate the overall contribution of the different winding set configurations subordinated to the overload capability in steady-state conditions.

As previously mentioned, the dc excitation allows at locating the heat source in the winding, and its heating power can be easy quantified. Moreover, as discussed by the authors in [16], the other heat sources like iron losses, rotor joule losses, etc. impose a thermal polarization at the stator winding temperature, but they do not change the time evolution of the machine temperature.

The dc steady-state test allows at directly assessing the thermal resistances within the machine body, where the thermal parameters (thermal conductivity, heat transfer coefficient, and geometrical dimensions) are not known precisely.

The temperature distribution within the machine has to be measured after reaching the thermal equilibrium, in particular, those related to the winding, stator core, housing, and ambient. It is worth to note that for the steady-state thermal test it has been assumed that the thermal equilibrium within the machine body is reached if the winding temperature rise is lower than 1°C over 30 min.

It should be remarked that, as for the transient test, the winding temperature has been estimated from the variation of

the winding resistance since it returns more reliable results to the sensors measurements. Indeed, it is important to underline that the temperature sensor measures a local temperature that depends on the sensor position. Conversely, a temperature measurement using the winding resistance returns an average temperature of the same. Besides, during the steady-state, the configuration of the winding sets for the investigated machine is the same as for the thermal transient tests, as depicted in Fig. 7.

Two test conditions have been investigated, assessing the steady-state overload capability in the open-fault winding configuration. The first one consists of feeding the machine with a current equal to the rated one. Conversely, for the second test, the machine is heated up at constant current values computed with (4-6) up to rated Joule losses, as shown in Figs. 21-24. The results of the experimental investigation are summarized in Table I and Table II. Looking at the measurements listed in Table I, it can be noted a significant difference in the steady-state overtemperature of the winding set when the machine is fed with a given current. As an example, the maximum temperature deviation is up to -35.7 °C for the case of a one-set configuration. This shows a potential overload capability when one or more three-phase sets are in open-fault.

The outlook is confirmed when the machine is heated up with the rated Joule losses. This value is measured in steady-state thermal conditions, by considering all the sets active and by injecting the rated current of the machine. Therefore, it can be expressed as:

$$P_{j,rated} = 4 \cdot \left(3 \cdot R_{ph,ss}\right) \cdot I_{rated}^2 \qquad (4)$$

where $P_{j,rated}$ is the value of rated Joule losses; $R_{ph,ss}$ is the resistance of each single-phase winding in steady-state conditions while I_{rated} is the rated current of the machine, corresponding to 10 A, as shown in Appendix, Table III.

Regardless of the number of active sets, the thermal resistance of the winding is negligible to the overall one (from winding to the external environment). Therefore, by heating the machine with the rated Joule losses, the overtemperature of the winding in the steady-state thermal condition is not affected by the number of active sets, leading to the following expression:

$$P_{j,rated} = n \cdot \left(3 \cdot R_{ph,ss}\right) \cdot I_{n,ovl}^2 \qquad (5)$$

where n is the number of active sets while $I_{n,ovl}$ is the overload current. In other words, the latter can be seen as the rated current of the machine in faulty conditions. By merging (4)-(5), the overload current $I_{n,ovl}$ is computed as:

$$I_{n,ovl} = \frac{2}{\sqrt{n}} \cdot I_{rated} \qquad (6)$$

The application of (6) leads to the results shown in Table II. It is noted how the steady-state overtemperature of the winding reaches approximatively the same value, with a measured maximum deviation of 4°C, resulting in acceptable considering the complexity of the system. Therefore, it is confirmed that the configuration of the winding sets has a negligible impact on the overall thermal path from the winding region to the ambient. Furthermore, it is noted how in steady-state operation, the mutual thermal coupling effect noted during the assessment of the transient tests is mitigated.

Fig. 21. Measured temperature variation during the steady-state thermal test (four active winding sets).

Fig. 22. Measured temperature variation during the steady-state thermal test (three active winding sets).
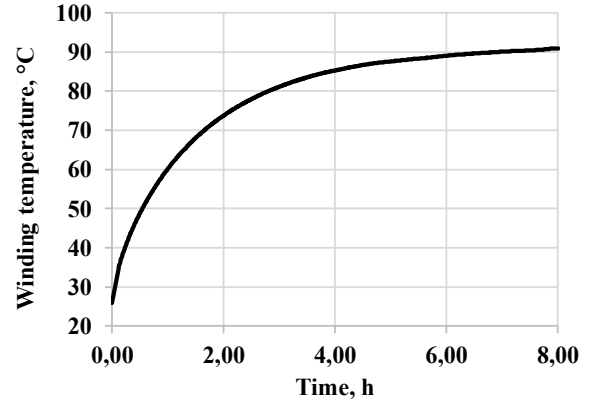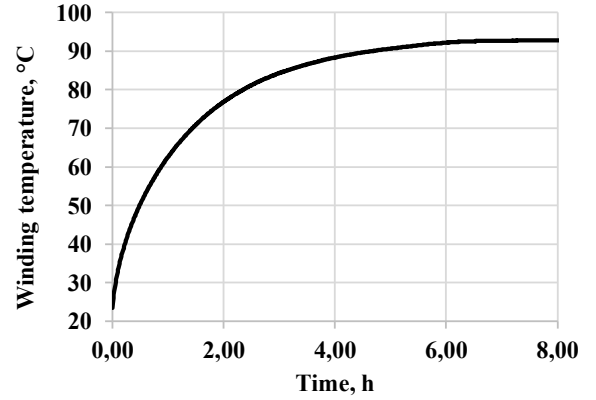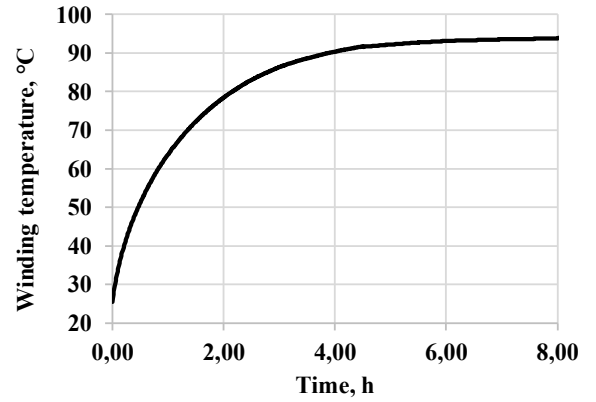

Fig. 23. Measured temperature variation during the steady-state thermal test (two active winding sets).
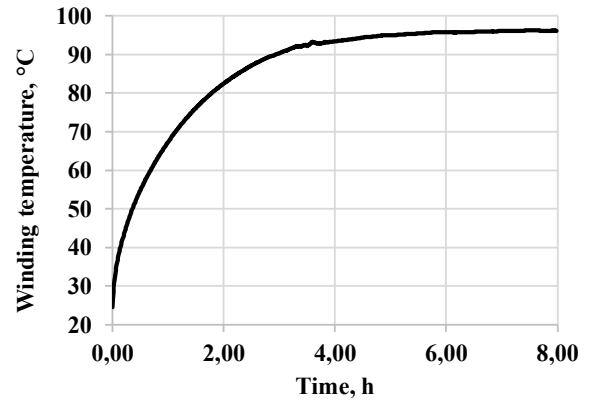

Fig. 24. Measured temperature variation during the steady-state thermal test (one active winding set).

TABLE I
STEADY-STATE STATOR WINDING TEMPERATURE AT RATED CURRENT.

	Four Sets	Three Sets	Two Sets	One Set
Current, A	10			
Joule Losses, W	220	183	100	49
Winding overtemperature, °C	65.2	61.2	38.2	29.5
Set temperature differences, °C	-	-4	-27.0	-35.7
Ambient temperature, °C	26	24.5	25.5	19

TABLE II
STEADY-STATE STATOR WINDING TEMPERATURE AT RATED LOSSES.

	Four Sets	Three Sets	Two Sets	One Set
Joule losses, W	220			
Current, A	10.0	11.5	14.1	20.0
Winding overtemperature, °C	67.5	65.8	63.4	64.1
Set temperature differences, °C	-	-1.7	-4.1	-3.4
Ambient temperature, °C	26	24	23	24

The results suggest that the machine may be overloaded with a current rating of 11.5 A, 14.1 A, and 20 A when three-sets, two-sets, and one-set are active, respectively. It is important to remark that the other heat sources would introduce a bias on the temperature distribution of the winding. The thermal test in operative condition has not been performed yet. However, as discussed in [19], the first order thermal model has been tested in operative conditions with good results on an industrial induction motor.

V. CONCLUSION

The paper addresses the thermal behavior of multiple three-phase machines under normal and open-phase fault conditions. In particular, the winding thermal model of a reduced scale multiphase induction machine prototype has been obtained, by considering the mutual heat exchange phenomena among the winding sets when one or more sets are disconnected.

The proposed procedure allows at obtaining the overload capability when one or more winding sets are turned off, for both steady-state and short transient operating conditions. The results can be used for the proper tuning of the current limit of the machine control scheme that must withstand "open-phase fault-ride through" capability if one or more inverter units are turned off in case of faults.

For the quadruple three-phase induction machine considered in the paper, the phase current may increase by 11.5%, 40%, and 95% when one set, two sets, and three sets are turned off, as demonstrated in Table II.

The paper demonstrated that the thermal capacitances of the set configurations could be computed using just one set. This feature is important when the multiphase machine cannot be tested with all sets due to physical constraints.
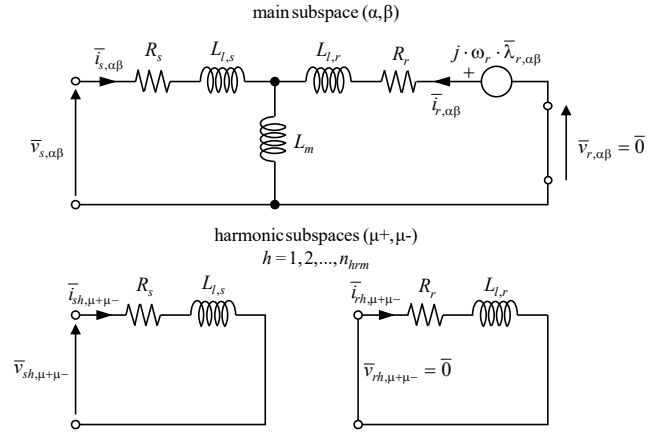

Fig. 25. Equivalent circuit of a multiphase induction machine using the VSD approach.

TABLE III
INDUCTION MACHINE RATED DATA.

Rated phase voltage	115 Vrms
Rated current	10 Arms
Rated power as a generator	10 kVA
Rated power factor	0.8
Pole pairs	2
Stator/rotor slots	48/40
Cooling system	Natural convection

TABLE IV
INDUCTION MACHINE RATED PARAMETERS.

Machine Parameters (Rated Value @ 25°C)	
Stator resistance R_s	145 mΩ
Stator leakage inductance L_{ls}	0.94 mH
Magnetizing inductance L_m	4.3 mH
Rotor resistance R_r	45 mΩ
Rotor leakage inductance L_{lr}	0.235 mH

APPENDIX

The multiphase machine prototype is a 12-phase induction machine designed for an open-rotor aero-engine as a starter-alternator [20]. The rated data and parameters are given in Table III and Table IV. The equivalent circuit of the machine using the Vector Space Decomposition (VSD) approach is shown in Fig. 25. More details about its meaning can be found in [21].

REFERENCES

[1] E. Levi, "Advances in Converter Control and Innovative Exploitation of Additional Degrees of Freedom for Multiphase Machines", *IEEE Trans. Ind. Electron.*, vol.63, no.1, 2016, pp.433-448.

[2] E. Levi, "Multiphase Electric Machines for Variable-Speed Applications", *IEEE Trans. Ind. Electron.*, vol. 55, no. 5, 2008.

[3] I. Gonzalez-Prieto, M.J. Duran, H.S. Che, E. Levi, and F. Barrero," Fault-Tolerant Operation of Six-Phase Energy Conversion Systems

With Parallel Machine-Side Converters", *IEEE Trans. Power Electron.*, vol. 31, no. 4, 2016, pp. 3068-3079.

[4] X. Huang, A. Goodman, C. Gerada, F. Youtong, and L. Qinfen, "Design of a Five-Phase Brushless DC Motor for a Safety Critical Aerospace Application", *IEEE Trans. Ind. Electron.*, vol. 59, no. 9, 2012.

[5] R. Bojoi, S. Rubino, A. Tenconi and S. Vaschetto, "Multiphase Electrical Machines and Drives:A Viable Solution for Energy Generation and Transportation Electrification", Conf. Rec. EPE, 2016, pp. 632-639.

[6] Y. Zhao, T.A. Lipo, "Modeling and control of a multi-phase induction machine with structural unbalance", *IEEE Trans. Energy Conversion*, 1996, vol.11, no.3, pp. 570-577.

[7] R. Kianinezhad, B. Nahid-Mobarakeh, L. Baghli, F. Betin and G.-A. Capolino, "Modeling and Control of Six-Phase Symmetrical Induction Machine Under Fault Condition Due to Open Phases", *IEEE Trans. Ind. Electron.*, vol. 55, no. 5, pp. 1966-1977, 2008.

[8] H.S. Che, M.J. Duran, E. Levi, M. Jones, W.P. Hew and N.A. Rahim, "Postfault Operation of an Asymmetrical Six-Phase Induction Machine With Single and Two Isolated Neutral Points", *IEEE Trans. Power Electron.*,vol. 29, no.10, pp. 5406-5416, 2014.

[9] R. Bojoi, A. Cavagnino, A. Tenconi, and S. Vaschetto, "Control of Shaft-Line-Embedded Multiphase Starter/Generator for Aero-Engine", *IEEE Trans. Ind. Electron.*, vol. 63,no. 1, 2016, pp. 641-652.

[10] L. Alberti, and N. Bianchi,"Experimental Tests of Dual Three-Phase Induction Motor Under Faulty Operating Conditions", *IEEE Trans. Ind. Electron.*, vol.59, no.5, pp. 2041-2048, 2012.

[11] L. Alberti, and N. Bianchi, "Impact of winding arrangement in dual 3-phase induction motor for fault tolerant applications", Conf. Rec. International Conf. on Electrical Machines (ICEM) 2010, pp. 1-6.

[12] N. Bianchi, E. Fornasiero, S. Bolognani, "Thermal Analysis of Five-Phase Motor Under Faulty Operation", *IEEE Trans. Ind. Appl.* Vol. 48. No. 4, 1531-1538, 2013

[13] H. Zahr, M. Trabelsi, E. Semail, "Comparison and Analysis of Post-Fault Operation Models in a five-Phase PMSM Considering Thermal Behavior", Conf. Proc. CPE Powereng, pp-1-6, 2018.

[14] A. Boglietti, R. Bojoi, S. Rubino and M. Cossale, "Load Capability of Multiphase Machines under Normal and Open-Phase Fault Conditions," 2018 IEEE Energy Conversion Congress and Exposition (ECCE), Portland, OR, 2018, pp. 242-247.

[15] https://www.motor-design.com/motor-cad-software/

[16] A. Boglietti, E. Carpaneto, M. Cossale, S. Vaschetto, M. Popescu, D. A. Staton, "Stator Winding Thermal Conductivity Evaluation: an Industrial Production Assessment" *IEEE Trans. Ind. Appl.*, vol. 52. No. 5, pp. 3893-3900, 2016.

[17] A. Boglietti, M. Cossale, S. Vaschetto, T. Dutra,"Thermal Conductivity Evaluation of Fractional-Slot Concentrated-Winding Machines", *IEEE Trans. Ind. Appl.*, Vol. 53, no. 3, pp. 2059-2065, 2017.

[18] A. Boglietti; E. Carpaneto; M. Cossale; S. Vaschetto, "Stator-Winding Thermal Models for Short-Time Thermal Transients: Definition and Validation", *IEEE Trans. on Ind. Electron.*, Year: 2016, Volume: 63, Issue: 5, Pages: 2713 – 2721.

[19] A. Boglietti; M. Cossale; S. Vaschetto; T. Dutra, "Winding Thermal Model for Short-Time Transient: Experimental Validation in Operative Conditions", *IEEE Trans. on Ind. Appl.*, Year: 2018 , Volume: 54, Issue: 2

[20] G. Rizzoli, G. Serra, P. Maggiore, A. Tenconi, "Optimized design of a multiphase induction machine for an open rotor aero-engine shaft- line-embedded starter/generator", IEEE ICEM, 2014, pp. 2107–2113.

[21] S. Rubino, R. Bojoi, A. Cavagnino and S. Vaschetto, "Asymmetrical twelve-phase induction starter/generator for more electric engine in aircraft," 2016 IEEE Energy Conversion Congress and Exposition (ECCE), Milwaukee, WI, 2016, pp. 1-8.